Available online at www.sciencedirect.com
ScienceDirect
Trans. Nonferrous Met. Soc. China 32(2022) 3578−3586
Transactions of Nonferrous Metals Society of China
www.tnmsc.cn

Microstructure and mechanical behavior of Ti−Cu alloys produced by semisolid processing

Kaio NIITSU CAMPO[1], Caio Chaussê de FREITAS[1], Éder Sócrates Najar LOPES[1], Suk-Chun MOON[2], Rian DIPPENAAR[2], Rubens CARAM[1]

1. School of Mechanical Engineering, University of Campinas, Campinas, SP, Brazil;
2. School of Mechanical, Materials, Mechatronic and Biomedical Engineering, University of Wollongong, Wollongong, NSW, Australia

Received 17 October 2021; accepted 21 February 2022

Abstract: The mechanical properties of Ti−Cu alloys processed via thixoforming were evaluated. Ti−Cu (25, 27, and 29 wt.% Cu) ingots were produced via arc melting, homogenization at 950 °C for 24 h, and hot-forging at 900 °C, followed by thixoforming at a speed of 8 mm/s after isothermal heat treatment at 1035 °C for 300 s. The thixoformed alloys exhibited good mechanical strength, limited plasticity under tensile loading, and reasonable plasticity under compressive loading. The mechanical strength and plasticity decreased as the Cu content increased as a result of the increasing volume fraction of the peritectic Ti_2Cu phase (transformed liquid), which exhibited a lower strength and plasticity than the $\alpha + Ti_2Cu$ regions (transformed solid). These findings indicated that the trade-off between the mechanical properties and semisolid processability is largely governed by the Cu content.
Key words: semisolid processing; thixoforming; Ti−Cu alloys; microstructure; mechanical properties

1 Introduction

The semisolid processing of alloys is an advanced method for manufacturing metallic components. It involves the use of raw materials in the semisolid state, and hence, offers advantages over conventional manufacturing processes in terms of controllable die/mold filling and high near-net-shape capability [1]. Ti−Cu alloys have been recognized as potential raw materials for semisolid processing [2−9]. When Cu is added to Ti, the liquidus and solidus temperatures decrease, while the semisolid interval increases, allowing for lower processing temperatures and reduced liquid fraction sensitivity, respectively. Thus, the higher the Cu content, the higher the achievable liquid fraction at lower temperatures [2]; this feature is highly beneficial, primarily with regard to energy consumption and the thermal impact on tools, molds, and dies. However, excess Cu significantly affects the resultant properties. The use of Cu as an alloying element in Ti has been reported to enhance grindability [10], wear resistance [11], antibacterial activity [12−14], and burn resistance [15,16]. However, the formation of Ti_2Cu intermetallics can lead to reduced ductility [17].

As bacterial infection is a major concern associated with the use of medical and dental implants, the development of Ti−Cu alloys for such applications has increased in recent years, owing to the antimicrobial properties of Cu [18]. Furthermore, Ti−Cu alloys exhibit reasonable biocompatibility. In a recent study, JAVADHESARI et al [13] revealed that in addition to the antibacterial activity against *E. coli* and *S. aureus*, a

Corresponding author: Kaio NIITSU CAMPO, Tel: +55-19-35213314, Fax: +55-19-32893722, E-mail: kaioniitsu@gmail.com
DOI: 10.1016/S1003-6326(22)66040-0

Ti−Cu alloy with a Cu content as high as ~57 wt.% displayed good biocompatibility. LIU et al [12] established that the Cu content should be ≥5 wt.% to provide efficacious antibacterial properties against the above-mentioned bacteria. Considering that Ti−Cu alloys specifically developed for semisolid processing contain Cu contents (between 25−29 wt.% [2]) within the range established by the above-mentioned studies [12,13], it is reasonable to assume that semisolid processing is a promising manufacturing route for the fabrication of antibacterial biomedical devices. However, the mechanical properties of these alloys have not yet been investigated. In addition to their composition, the mechanical performance of Ti−Cu alloys depends on the processing conditions [19]. Therefore, in this study, the mechanical properties of thixoformed Ti−Cu alloys are evaluated.

2 Experimental

Ti−Cu (25, 27, and 29 wt.% Cu) ingots were produced by arc melting, homogenization at 950 °C for 24 h, and hot-forging (swaging) at 900 °C, and were then machined to a final diameter of 10 mm [5]. A simple thixoforming process (forging system) was performed under argon atmosphere using the experimental apparatus shown in Fig. 1(a) [8]. Figure 1(b) shows a schematic of the die, which has a recess with an isosceles trapezoidal section. Thixoforming was performed at a rate of 8 mm/s after isothermal heat treatment at 1035 °C for 300 s. The temperature was controlled using an optical pyrometer (disappearing-filament-type, CHINO IR-U) previously calibrated against type-K thermocouples [8]. The edges of the samples were heated to a higher temperature because they were closer to the induction coil. However, only the middle sections of the samples were analyzed. At 1035 °C, the liquid fractions of Ti−25Cu, Ti−27Cu, and Ti−29Cu were approximately 0.27, 0.37, and 0.46, respectively [5].

The microstructural characterization was performed using scanning electron microscopy (SEM, FEI Quanta 650 FEG), X-ray diffraction (XRD; PANalytical X'Pert, Cu K_α radiation), and high-temperature laser-scanning confocal microscopy (HT-LSCM, Lasertec Corp. [6]). Vickers hardness measurements were performed using a Buehler Micromet 2100 tester (4.9 N for 10 s) and a nanoindentation tester (NHT−CSM Instruments) equipped with a Berkovich indenter (0.0098 N for 10 s). Tensile tests were conducted using flat, miniaturized, dogbone-shaped specimens (gauge length, width, and thickness of 7, 1.8, and 1 mm, respectively). These specimens were extracted via wire electric discharge machining, where the face of the tensile specimens was parallel to the plane formed by the x and z directions (Fig. 1(b)). From each thixoformed sample, four to five specimens were obtained for the tensile tests, conducted at a constant speed of 0.2 mm/min using a Deben Microtest 5000 N tensile stage. Compression tests were also conducted using cylindrical specimens (d2 mm × 4 mm). The longitudinal direction of the specimen was parallel to z-direction (Fig. 1(b)). Seven to ten specimens of each alloy were tested using a universal testing machine (Emic DL2000) at a constant speed of 2 mm/min. Statistical analysis was performed based on analysis of variance (ANOVA) and Tukey's test with α=0.05.

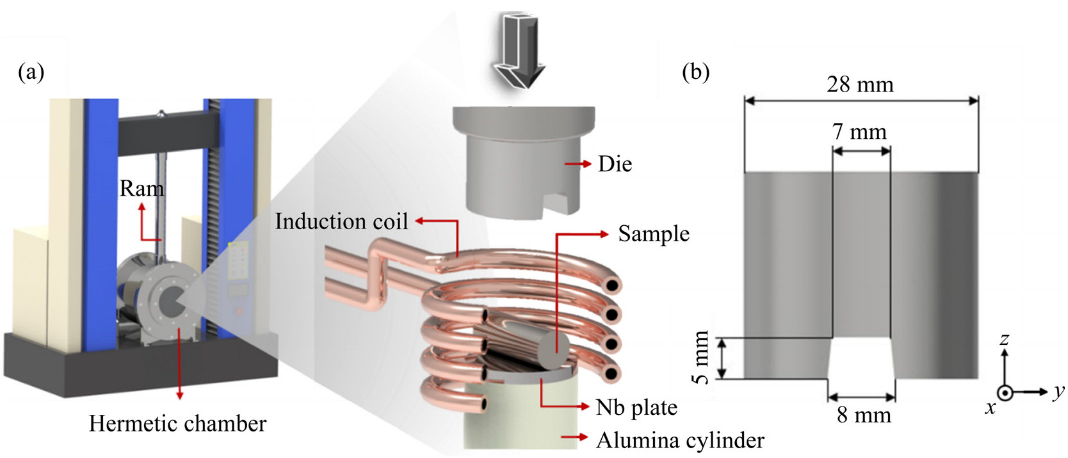

Fig. 1 Schematic of thixoforming experimental apparatus (a) and die cross-section (b)

3 Results and discussion

3.1 Thixoformed samples

The representative macroscopic appearances of the thixoformed samples after burr removal are shown in Fig. 2. The material did not react with the die and no visible oxidation had occurred, irrespective of the liquid content in the raw material, which increased with increasing Cu content. Some surface cracks were observed, mainly at the tips and edges of the thixoformed Ti−25Cu alloy. During deformation under unconstrained conditions, the tendency for crack formation in semisolid alloys increases with a decreasing liquid fraction [20]. This explains the higher crack concentration at the tips of the samples; deformation of the semisolid sample occurs more readily in these regions due to the die design (Fig. 1(b)).

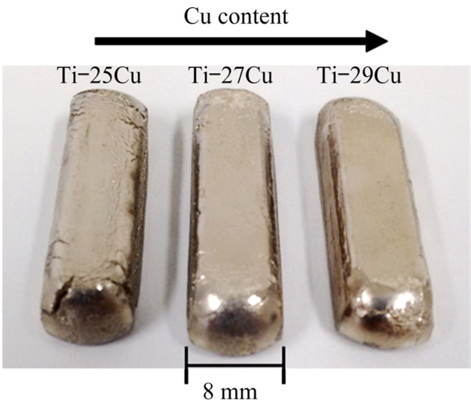

Fig. 2 Representative macroscopic image of thixoformed samples after burr removal

3.2 Microstructure

SEM-backscattered electron (SEM-BSE) images of the microstructures of the thixoformed samples are shown in Figs. 3(a−c). In these micrographs, the transformed liquid is represented by the light matrix, whereas the transformed solid is represented by the dark particles. As expected, the liquid fraction increased with increasing Cu content. Based on image analysis, the transformed liquid fractions in volume (or in area) were determined to be ~0.30, 0.40, and 0.46, with increasing Cu content. Regardless of the alloy composition, the microstructure can be classified as globular, as the shape of the majority of the solid particles closely resembled that of an ideal circle observed when particles with globular morphology are investigated

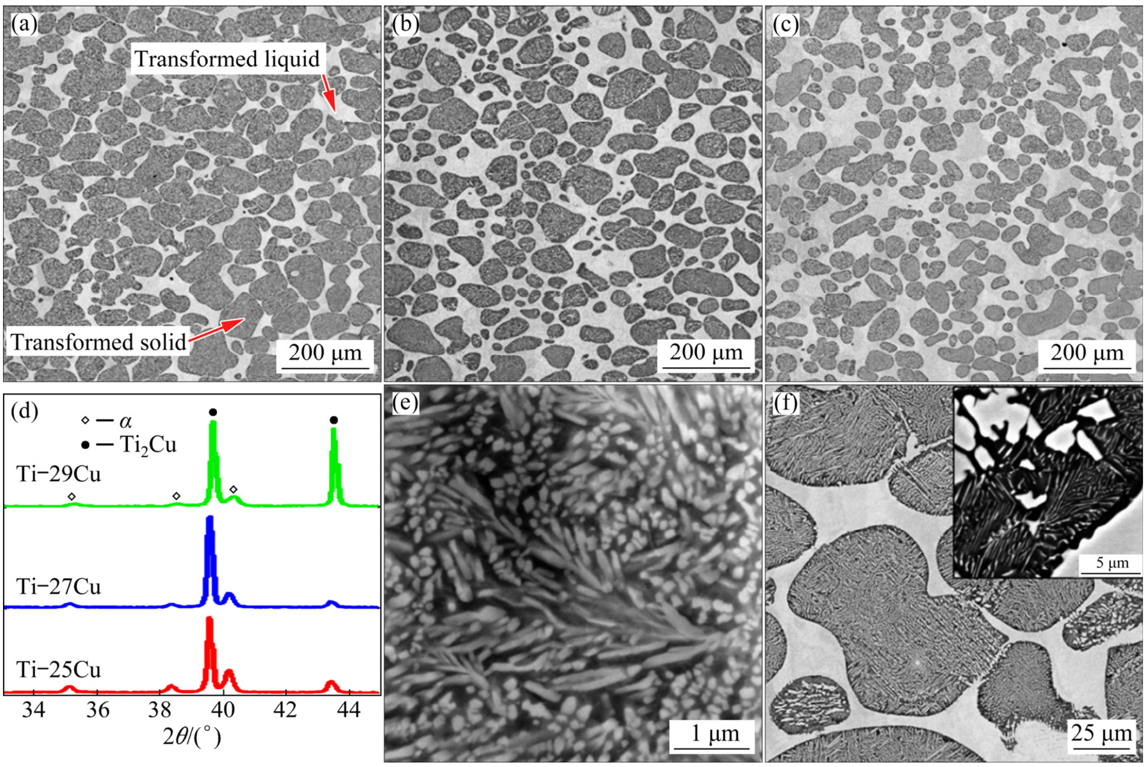

Fig. 3 Typical SEM-BSE images of microstructures of thixoformed Ti−25Cu (a), Ti−27Cu (b) and Ti−29Cu (c); XRD patterns of thixoformed alloys (d); Detailed view of transformed solid region (α + Ti_2Cu) after water quenching (e) and thixoforming (f)

using planar sections. Globularization commenced with the recrystallization of the deformed dendrites during hot forging and subsequent heating to the semisolid state. The fraction of high-angle boundaries increased after recrystallization. Therefore, the microstructure could be efficiently shattered during liquid formation, generating small solid particles that could be rapidly globularized during isothermal heat treatment (300 s) prior to thixoforming [5]. The thixoformed microstructures were composed solely of the α and Ti_2Cu phases, as confirmed by the XRD results shown in Fig. 3(d). The Ti−Cu system exhibits an active eutectoid transformation. In this case, β-phase decomposition cannot be avoided even with rapid quenching, as previously demonstrated in studies employing hypereutectoid Ti−Cu alloys [5,21,22]. Therefore, the dark regions in Figs. 3(a−c) represent a mixture of the α and Ti_2Cu phases (Fig. 3(e)). The morphology of the products resulting from β-phase decomposition is dependent on the cooling rate [21,22]. During solidification, the semisolid microstructure forms grains of the β phase surrounded by the peritectic Ti_2Cu phase. As the temperature decreases, the Ti_2Cu fraction increases while the β phase fraction decreases and becomes poorer in Cu until eutectoid transformation of the remaining β phase occurs (Fig. 4). However, high cooling rates, such as those encountered in water quenching, suppress equilibrium phase fraction evolution; consequently, the decomposition of the supersaturated β phase generates very fine Ti_2Cu particles within the α matrix (Fig. 3(e)) [5]. Because of the lower cooling rate during thixoforming, blocky nodules and laths of proeutectoid Ti_2Cu were observed in some regions. The blocky precipitates were formed at the boundary between the β and Ti_2Cu phases and inside the β grains. Colonies of the lamellar eutectoid ($\alpha + Ti_2Cu$) formed around the Ti_2Cu blocks (inset of Fig. 3(f)) following the eutectoid transformation [21]. In regions where blocky Ti_2Cu did not form, β-phase decomposition led to the formation of Ti_2Cu precipitates that resembled those observed after water quenching (Fig. 3(e)); however, they were much coarser owing to the lower cooling rate.

Microstructure formation was further studied using HT-LSCM. In-situ observations were performed for the hot-forged Ti−25Cu alloy, which was cyclically heated to 950 °C and then cooled at varying cooling rates. Figure 5(a) shows the microstructure evolution at a cooling rate of 500 °C/min. At 950 °C, the microstructure is formed by β grains and peritectic Ti_2Cu. As the temperature decreased, Ti_2Cu laths formed and grew, as shown in the micrograph obtained at 850 °C (Fig. 5(a)). At this cooling rate, the first Ti_2Cu lath was observed at approximately 870 °C. Upon slow cooling, in addition to coarser Ti_2Cu particles (Figs. 5(b, c)), the first Ti_2Cu laths appeared at higher temperatures, at approximately 900 and 920 °C for cooling rates of 100 and 50 °C/min, respectively. Although the discrepancy exists between the temperature on the sample surface and the temperature shown by the control thermocouple [6], it was not considered to be significant. For instance, liquid formation of this sample occurred at approximately 980 °C, while the equilibrium peritectic temperature is ~990 °C (Fig. 4). Therefore, as shown in Fig. 5, the first Ti_2Cu laths formed during cooling must have been generated as a proeutectoid product, because the equilibrium eutectoid temperature is close to 800 °C (Fig. 4). These observations strongly indicate that the blocky nodules and laths of Ti_2Cu were formed before the eutectic temperature was reached with cooling during thixoforming.

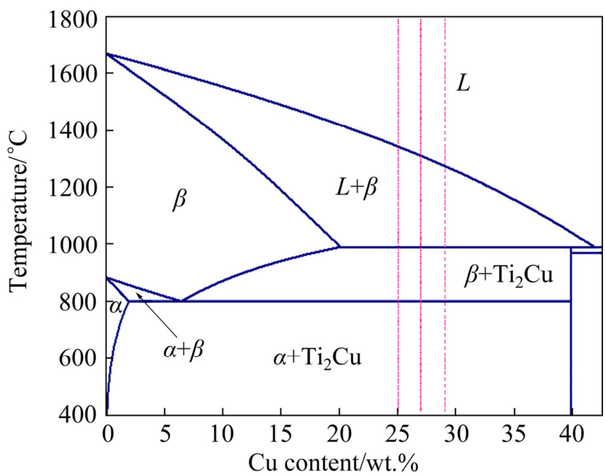

Fig. 4 Phase diagram of Ti−Cu system [2,29]

3.3 Mechanical properties

The mechanical properties of the alloy samples are summarized in Table 1. The obtained Vickers hardness mean and standard deviation values were (302±15), (292±15), and (291±9) HV for thixoformed Ti−25Cu, Ti−27Cu, and Ti−29Cu, respectively. ANOVA revealed that the mean values

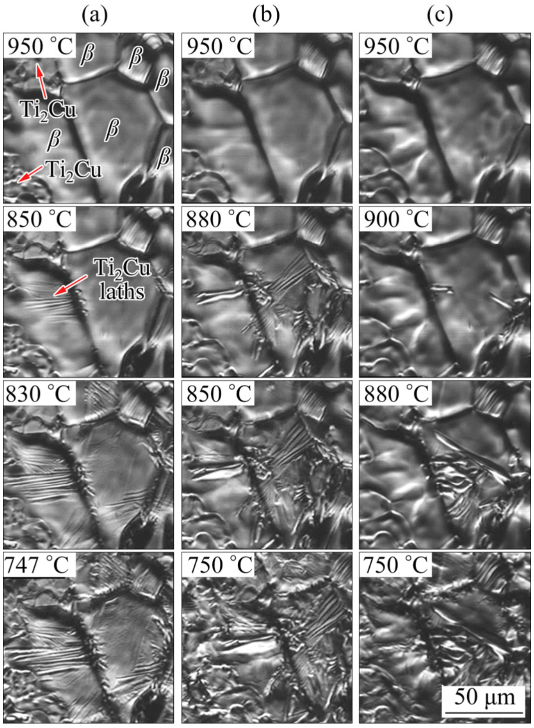

Fig. 5 In-situ HT-LSCM images of microstructure of hot-forged Ti−25Cu cyclically heated to 950 °C and cooled at 500 (a), 100 (b), and 50 °C/min (c)

were not statistically different (p>0.05). Although the volume fractions of the transformed liquid and solid changed according to the composition, the samples exhibited similar hardness values, suggesting that their local hardness properties were comparable. To confirm this, nanoindentation measurements were performed for each specific region in the Ti−29Cu sample. Again, ANOVA revealed that the hardness values of the transformed liquid and solid regions were not statistically different (p>0.05), with the mean and standard deviation values of (298±16) and (299±11) HV, respectively. The tensile behavior of an alloy can better describe its mechanical properties. Figure 6(a) presents the stress−strain curves of the thixoformed Ti−Cu alloys, while Fig. 6(b) shows the obtained mean and standard deviation values for the ultimate tensile strength (UTS) and elongation at fracture. As the Cu content decreased, the UTS and elongation increased (p<0.05); the UTS values were (870±66), (737±55), and (656±50) MPa for the Ti−25Cu, Ti−27Cu, and Ti−29Cu alloys, respectively. Note that the absolute values for elongation at fracture should be considered carefully, as an extensometer was not used for the miniaturized specimens. Therefore, the compliance of the testing device influenced the measurement, conveying overestimated results [23]. Interestingly, the tensile yield stress (0.2% proof stress) could not be determined because of the lack of linearity in the elastic region. Although this phenomenon occurs in some martensitic Ti alloys [24], it has not been observed in Ti−Cu alloys to date. Furthermore, the expected linear elastic behavior was observed under compression loading (shown later). Accordingly, the deviation in linearity was surmised to be related to the characteristics of the tensile testing device employed.

Figure 6(c) shows a typical fracture surface of the tested samples. Brittle fracture features can be observed, including the presence of cleavage planes and secondary cracks. However, under higher magnification (Fig. 6(d)), dimples are observed in some regions, which is the evidence of plastic deformation. Notably, with increasing Cu content, the number of dimpled regions decreased, which was expected based on the tensile test results shown

Table 1 Mean and standard deviation values for hardness, tensile, and compression properties of thixoformed Ti−Cu alloys

Test	Property	Ti−25Cu	Ti−27Cu	Ti−29Cu
Hardness	Vickers hardness ($HV_{0.5}$)	302±15^{a}	292±15^{a}	291±9^{a}
Tensile	Yield strength/MPa	−*	−*	−*
	Ultimate tensile strength/MPa	870±66^{a}	737±55^{bc}	656±50^{c}
	Elongation/%	7.2±0.6^{a}	4.8±0.8^{bc}	3.9±0.7^{c}
Compression	Yield strength/MPa	990±33^{a}	932±35^{ab}	865±65^{b}
	Compressive strength/MPa	1980±175^{a}	1765±125^{bc}	1690±116^{c}
	Plastic deformation/%	22.2±4.6^{a}	20.6±3.5^{a}	18.9±3.1^{a}

*Determination not possible; Mean values accompanied by the same letters are not statistically different (Tukey test, α = 0.05).

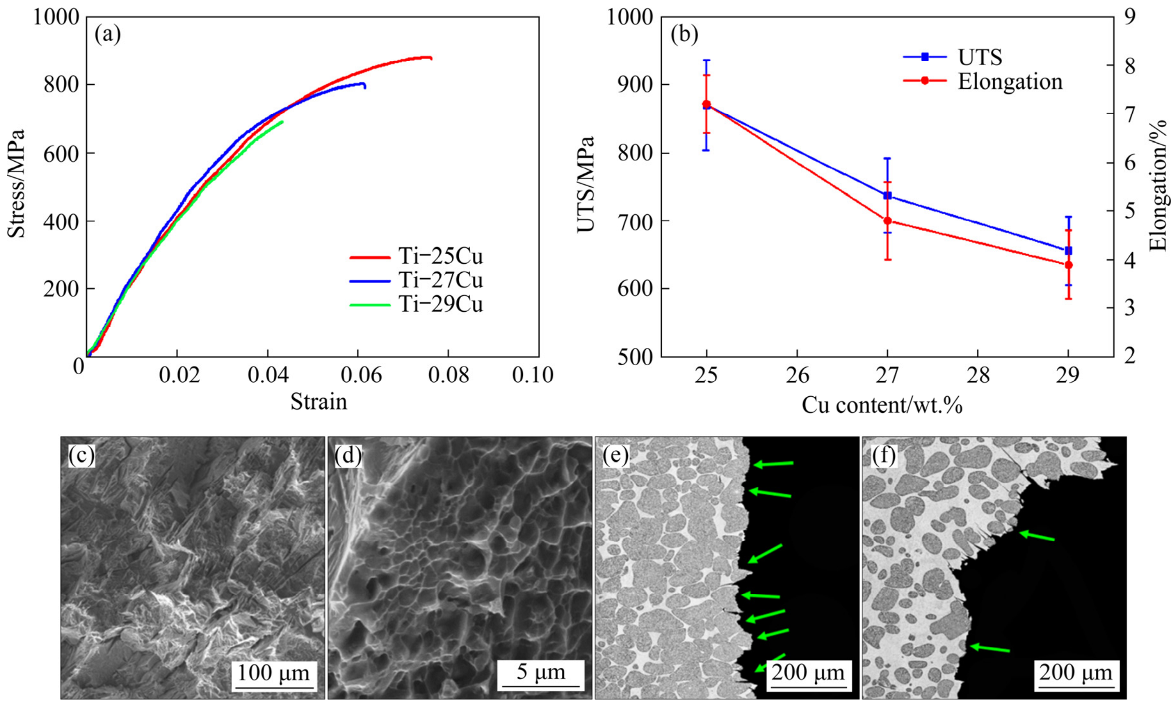

Fig. 6 Typical stress−strain curves obtained employing tensile tests (a); Ultimate tensile strength (UTS) and elongation at fracture, measured employing tensile tests (b); Typical fracture surfaces (c, d); Cross-sectional micrographs of Ti−25Cu (e) and Ti−29Cu (f) fractured tensile specimens

in Fig. 6(a). Crack progression during fracture in Ti−25Cu and Ti−29Cu is shown in Figs. 6(e) and (f), respectively. A fracture can occur via three routes in these alloys: (1) cleavage of the peritectic Ti_2Cu intermetallic compound (transformed liquid), (2) intergranular fracture occurring between the transformed solid and liquid regions, and (3) transgranular fracture occurring within the transformed solid regions (arrows). Only the transgranular fracture can be associated with dimple formation (Fig. 6(d)), because the crack passes through the higher-ductility phase (α phase). Therefore, as Ti−25Cu contained the highest volume fraction of transformed solid (~0.70), the probability of the crack passing through it was high, explaining its higher ductility.

Owing to the aforementioned limitations associated with the tensile tests, the thixoformed samples were additionally mechanically evaluated by compression tests. Figure 7(a) shows the typical compressive stress−strain curves for the Ti−25Cu, Ti−27Cu, and Ti−29Cu alloys. The mechanical strength decreased with increasing Cu content, in agreement with the tensile test results (Fig. 7(b)). The compression yield stress (0.2% proof stress) increased from (865±65) to (990±33) MPa ($p<0.05$), and the compressive strength increased from (1690±116) to (1980±175) MPa ($p<0.05$) when the Cu content decreased from 29 to 25 wt.%. On the other hand, the differences in the plastic deformation values obtained under compressive loading were not statistically significant ($p>0.05$), although a decreasing trend was observed with increasing Cu content; the mean and standard deviation values were (22.2±4.6), (20.6±3.5), and (18.8±3.1)% for Ti−25Cu, Ti−27Cu, and Ti−29Cu alloys, respectively, indicating good plasticity under compression.

Both the strength and plasticity appeared to increase with decreasing Cu content. The mechanical strength of these alloys seems to be more associated with the transformed solid region than the transformed liquid region. This is attributed to the biphasic structure ($\alpha + Ti_2Cu$) of the transformed solid region, which impairs dislocation motion more efficiently. The transformed liquid region is composed of the Ti_2Cu phase, which exhibits low mechanical strength. CHENG et al [25] conducted compression tests to determine the mechanical properties of the Ti_2Cu intermetallics and obtained a compression yield stress of only 416 MPa. Accordingly, when the Cu content

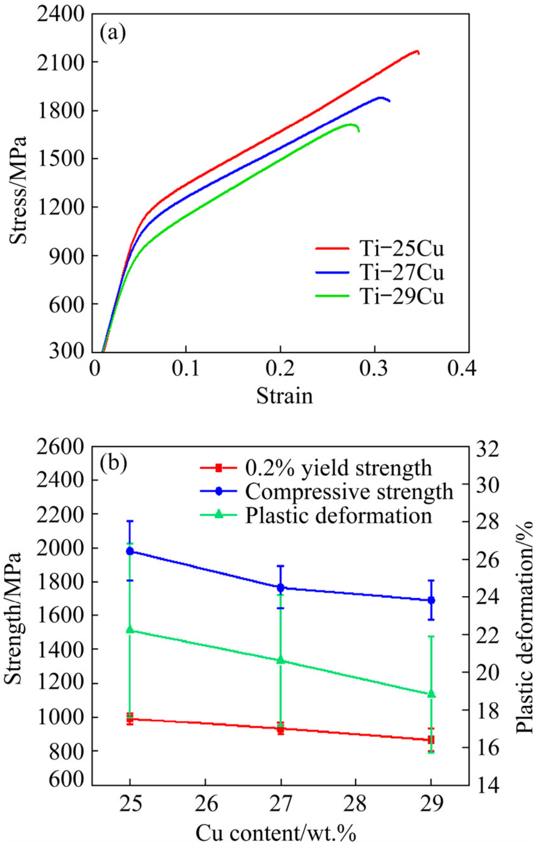

Fig. 7 Stress−strain curves obtained by compression tests (a); Yield and compressive strength, and plastic deformation obtained by compression tests (b)

increased, the transformed solid fraction decreased, thereby reducing the overall mechanical strength. Interestingly, despite presenting differing mechanical strengths, the hardness of the transformed liquid and solid region was comparable. This indicates that these regions do not share a similar strength−hardness relationship. On the other hand, plasticity is limited by the amount of Ti_2Cu present in the microstructure; that is, an increase in the Cu content in Ti-rich alloys tends to reduce the plasticity. The unfavorable impact of the Ti_2Cu intermetallics on plasticity has also been observed in Ti−Cu alloys with considerably lower Cu content [26−28].

By comparing the studied compositions, it can be concluded that Ti−29Cu exhibits higher thixoformability at 1035 °C than Ti−25Cu, owing to its higher liquid fraction, which leads to lower forming loads and reduced probability of defect formation [8]. However, its higher Cu content also results in the deterioration of mechanical properties. The Ti−25Cu alloy can show the same liquid fraction as the Ti−29Cu alloy, leading to similar rheological behavior. However, for this to occur, the processing temperature must be increased by approximately 115 °C (Fig. 8), increasing the reactivity of the alloy as well as energy consumption. Therefore, it is necessary to select compositions that exhibit a good balance between processability and the final mechanical properties required for a specific application.

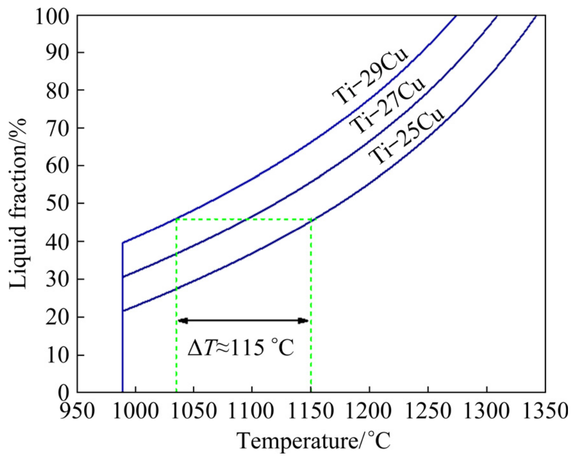

Fig. 8 Liquid fraction as function of temperature for Ti−25Cu, Ti−27Cu, and Ti−29Cu alloys (calculated at equilibrium [2,29])

4 Conclusions

(1) The thixoformed Ti−Cu alloys fabricated in this study exhibited a typical globular microstructure, comprising only α and Ti_2Cu phases, regardless of the Cu content.

(2) The alloys exhibited good mechanical strength, limited plasticity under tensile loading, and reasonable plasticity under compressive loading.

(3) Although the thixoformability at 1035 °C increased with increasing Cu content (higher liquid fraction), the mechanical strength and plasticity decreased, signifying a trade-off between the mechanical properties and semisolid processability. This occurred because an increase in the amount of Cu led to an increase in the volume fraction of the transformed liquid (peritectic Ti_2Cu), which is less ductile and weaker than the transformed solid regions ($\alpha + Ti_2Cu$).

Acknowledgments

This study was supported by the Brazilian research funding agencies FAPESP (São Paulo

Research Foundation), under the grant numbers 2013/24786–3 and 2017/07040–9, and CAPES (Federal Agency for the Support and Improvement of Higher Education). The authors also acknowledge the Villares Metals for donating high-purity Cu and the Brazilian Nanotechnology National Laboratory (LNNano/Cnpem) for access to the SEM facilities.

References

[1] ATKINSON H V. Semisolid processing of metallic materials [J]. Materials Science and Technology, 2010, 26: 1401−1413. https://doi.org/10.1179/026708310X12815992418012.

[2] CAMPO K N, de LIMA D D, LOPES É S N, CARAM R. On the selection of Ti−Cu alloys for thixoforming processes: Phase diagram and microstructural evaluation [J]. Journal of Materials Science, 2015, 50: 8007−8017. https://doi.org/10.1007/s10853-015-9367-4.

[3] CHEN Yong-nan, LUO Chuang, HUO Ya-zhou, BAI Fan, ZHAO Yong-qing, MA Xue-dan. Effect of Cu concentration on the semi-solid deformation behavior and microstructure of Ti−Cu alloy [J]. Advances in Mechanical Engineering, 2015, 7: 1687814015587428. https://doi.org/10.1177/1687814015587428.

[4] CHEN Yong-nan, HUO Ya-zhou, ZHAO Yi-ping, SONG Xu-ding, ZHAO Yong-qing, BI Zhao-zhao, LI Liao. Effect of Cu content on the semi-solid formability and mechanical properties of Ti−Cu alloys [J]. Rare Metal Materials and Engineering, 2016, 45: 1406−1412. https://doi.org/10.1016/S1875-5372(16)30122-9.

[5] CAMPO K N, LOPES É S N, PARRISH C H, CARAM R. Rapid quenching of semisolid Ti−Cu alloys: Insights into globular microstructure formation and coarsening [J]. Acta Materialia, 2017, 139: 86−95. https://doi.org/10.1016/j.actamat.2017.08.006.

[6] CAMPO K N, de FREITAS C C, MOON S C, DIPPENAAR R, CARAM R. In-situ microstructural observation of Ti−Cu alloys for semi-solid processing [J]. Materials Characterization, 2018, 145: 10−19. https://doi.org/10.1016/j.matchar.2018.08.016.

[7] de FREITAS C C, CAMPO K N, CARAM R. Thixoforming of titanium: The microstructure and processability of semisolid Ti−Cu−Fe alloys [J]. Vacuum, 2020, 180: 109567. https://doi.org/10.1016/j.vacuum.2020.109567.

[8] CAMPO K N, de FREITAS C C, CARAM R. Observations on the compression properties of semisolid Ti−Cu alloys [J]. Journal of Materials Research and Technology, 2020, 9: 15802−15810. https://doi.org/10.1016/j.jmrt.2020.11.014.

[9] ZHAO Dong, CHEN Yong-nan, JIANG Chao-ping, LI Yao, ZHAO Qin-yang, XU Yi-ku, ZHAN Hai-fei, WAN Ming-pan, ZHAO Yong-qing. Morphological evolution of Ti_2Cu in Ti−13Cu−Al alloy after cooling from semi-solid state [J]. Journal of Alloys and Compounds, 2020, 848: 156639. https://doi.org/10.1016/j.jallcom.2020.156639.

[10] KIKUCHI M, TAKADA Y, KIYOSUE S, YODA M, WOLDU M, CAI Z, OKUNO O, OKABE T. Grindability of cast Ti−Cu alloys [J]. Dental Materials, 2003, 19: 375−381. https://doi.org/10.1016/S0109-5641(02)00080-5.

[11] OHKUBO C, SHIMURA I, AOKI T, HANATANI S, HOSOI T, HATTORI M, ODA Y, OKABE T. Wear resistance of experimental Ti−Cu alloys [J]. Biomaterials, 2003, 24: 3377−3381. https://doi.org/10.1016/S0142-9612(03)00157-1.

[12] LIU Jie, LI Fang-bing, LIU Cong, WANG Hong-ying, REN Bao-rui, YANG Ke, ZHANG Er-lin. Effect of Cu content on the antibacterial activity of titanium−copper sintered alloys [J]. Material Science and Engineering C, 2014, 35: 392−400. https://doi.org/10.1016/j.msec.2013.11.028.

[13] JAVADHESARI S M, ALIPOUR S, AKBARPOUR M R. Biocompatibility, osseointegration, antibacterial and mechanical properties of nanocrystalline Ti−Cu alloy as a new orthopedic material [J]. Colloids and Surfaces B, 2020, 189: 110889. https://doi.org/10.1016/j.colsurfb.2020.110889.

[14] JI Hai-rui, ZHAO Ming-chun, XIE Bin, ZHAO Ying-chao, YIN Deng-feng, GAO Cheng-de, SHUAI Ci-jun, ATRENS Andrej. Corrosion and antibacterial performance of novel selective-laser-melted (SLMed) Ti−*x*Cu biomedical alloys [J]. Journal of Alloys and Compounds, 2021, 864: 158415. https://doi.org/10.1016/j.jallcom.2020.158415.

[15] ZHU K Y, ZHAO Y Q, QU H L, WU Z L, ZHAO X M. Microstructure and properties of burn-resistant Ti−Al−Cu alloys [J]. Journal of Materials Science, 2000, 35: 5609−5612. https://doi.org/10.1023/A:1004873501005.

[16] YANG Wen-qing, CHEN Yong-nan, ZHAO Qin-yang, ZHAN Hai-fei, XU Yi-ku, ZHANG Feng-ying, ZHAO Yong-qing, GU Yuan-tong. Multiscale exploit the role of copper on the burn resistant behavior of Ti−Cu alloy [J]. Journal of Alloys and Compounds, 2021, 863: 158639. https://doi.org/10.1016/j. jallcom.2021.158639.

[17] XU Yi-ku, JIANG Jian-li, YANG Ze-hui, ZHAO Qin-yang, CHEN Yong-nan, ZHAO Yong-qing. The effect of copper content on the mechanical and tribological properties of hypo-, hyper- and eutectoid Ti−Cu alloys [J]. Materials, 2020, 13: 3411. https://doi.org/10.3390/ma13153411.

[18] WANG Chun-ming, ZENG Lu-ming, DING Wu-cheng, LIANG Tong-xiang. Novel fabrication of low-cost Ti−Cu alloy by electroless copper plating and vacuum sintering [J]. Vacuum, 2021, 191: 110330. https://doi.org/10.1016/j.vacuum.2021.110330.

[19] ALSHAMMARI Y, YANG F, BOLZONI L. Low-cost powder metallurgy Ti−Cu alloys as a potential antibacterial material [J]. Journal of the Mechanical Behavior of Biomedical Materials, 2019, 95: 232−239. https://doi.org/10.1016/j.jmbbm.2019.04.004.

[20] KAREH K M, LEE P D, ATWOOD R C, CONNOLLEY T, GOURLAY C M. Revealing the micromechanisms behind semi-solid metal deformation with time-resolved X-ray tomography [J]. Nature Communications, 2016, 5: 1−7. https://doi.org/10.1038/ncomms5464.

[21] DONTHULA H, VISHWANADH B, ADAM T, BORKAR T, CONTIERI R J, CARAM R, BANERJEE R, TEWARI R, DEY G K, BANERJEE S. Morphological evolution of transformation products and eutectoid transformation(s) in a hyper-eutectoid Ti−12at.%Cu alloy [J]. Acta Materialia, 2019, 168: 63−75. https://doi.org/10.1016/j.actamat.2019.01.044.

[22] ZHAO Dong, CHEN Yong-nan, JIANG Chao-ping, LI Yao, ZHAO Qin-yang, XU Yi-ku, ZHAN Hai-fei, WAN Ming-pan, ZHAO Yong-qing. Morphological evolution of Ti_2Cu in Ti−13Cu−Al alloy after cooling from semi-solid state [J]. Journal of Alloys and Compounds, 2020, 848: 156639. https://doi.org/10.1016/j.jallcom.2020.156639.

[23] AKBARY F H, SANTOFIMIA M J, SIETSMA J. Elastic strain measurement of miniature tensile specimens [J]. Experimental Mechanics, 2014, 54: 165−173. https://doi.org/10.1007/s11340-013-9785-7.

[24] BÖNISCH M, CALIN M, van HUMBEECK J, SKROTZKI W, ECKERT J. Factors influencing the elastic moduli, reversible strains and hysteresis loops in martensitic Ti−Nb alloys [J]. Material Science and Engineering C, 2015, 48: 511−520. https://doi.org/10.1016/j.msec.2014.12.048.

[25] CHENG Jia-lin, YUN Ye-ling, WANG Jing-jing, RUI Jia-xin, WANG Shun, DU Yu-lei. Effect of Nb on the microstructure and mechanical properties of Ti_2Cu intermetallic through the first-principle calculations and experimental investigation [J]. Metals, 2020, 10: 547. https://doi.org/10.3390/met10040547.

[26] TAKAHASHI M, KIKUCHI M, TAKADA Y, OKUNO O. Mechanical properties and microstructures of dental cast Ti−Ag and Ti−Cu [J]. Dental Materials, 2002, 21: 270−280. https://doi.org/10.4012/dmj.21.270.

[27] KIKUCHI M, TAKADA Y, KIYOSUE S, YODA M, WOLDU M, CAI Z, OKUNO O, OKABE T. Mechanical properties and microstructures of cast Ti−Cu alloys [J]. Dental Materials, 2013, 19: 174−181. https://doi.org/10.1016/S0109-5641(02)00027-1.

[28] HAYAMA A O F, ANDRADE P N, CREMASCO A, CONTIERI R J, AFONSO C R M, CARAM R. Effects of compositions and heat treatment on the mechanical behavior of Ti−Cu alloys [J]. Materials & Design, 2014, 55: 1006−1013. https://doi.org/10.1016/j.matdes.2013.10.050.

[29] KUMAR K C H, ANSARA I, WOLLANTS P, DELAEY L. Thermodynamic optimization of the Cu−Ti system [J]. International Journal of Materials Research, 1996, 87: 666−672. https://doi.org/10.1515/ijmr-1996-870811.

半固态加工 Ti−Cu 合金的显微组织和力学行为

Kaio NIITSU CAMPO[1], Caio Chaussê de FREITAS[1], Éder Sócrates Najar LOPES[1],
Suk-Chun MOON[2], Rian DIPPENAAR[2], Rubens CARAM[1]

1. School of Mechanical Engineering, University of Campinas, Campinas, SP, Brazil;
2. School of Mechanical, Materials, Mechatronic and Biomedical Engineering,
University of Wollongong, Wollongong, NSW, Australia

摘　要：研究触变成形 Ti−Cu 合金的力学性能。Ti−Cu (25%，27%，29% Cu，质量分数) 锭的制备流程为：先进行电弧熔炼，再在 950 ℃均匀化处理 24 h，然后在 900 ℃热锻，最后在 1035 ℃热处理 300 s 后以 8 mm/s 的速度触变成形。结果显示，触变成形合金表现出良好的力学强度，但其在拉伸载荷下的塑性一般，在压缩载荷下的塑性尚可。随着 Cu 含量的增加，包晶 Ti_2Cu 相(转变液相区)的体积分数增加，与 α+Ti_2Cu 相区(转变固相区)相比，其力学强度和塑性更低，导致合金的力学强度和塑性降低。这些结果表明，Ti−Cu 合金的力学性能和半固态加工性之间的平衡主要取决于 Cu 含量。

关键词：半固态加工；触变成形；Ti−Cu 合金；显微组织；力学性能

(Edited by Bing YANG)